

## Supplementary Information

### **A novel vanadium Coordination Supramolecular Network with multiple active-sites for ultra-durable aqueous zinc metal batteries**

Shimei Lai <sup>1</sup>, Zengren Tao <sup>1</sup>, Jiawei Cui, Anding Wang, Yuanming Tan, Zhao Chen, Yangyi Yang

\*

School of Materials Science and Engineering, Sun Yat-sen University, Guangzhou 510275, PR  
China.

\*Corresponding author. E-mail: cesyyy@mail.sysu.edu.cn

Shimei Lai and Zengren Tao contributed equally to this work.

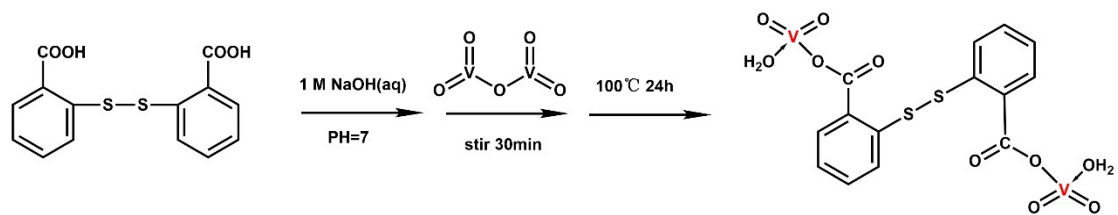


**Fig. S1.** Schematic illustration of the preparation procedure of V-CSN.

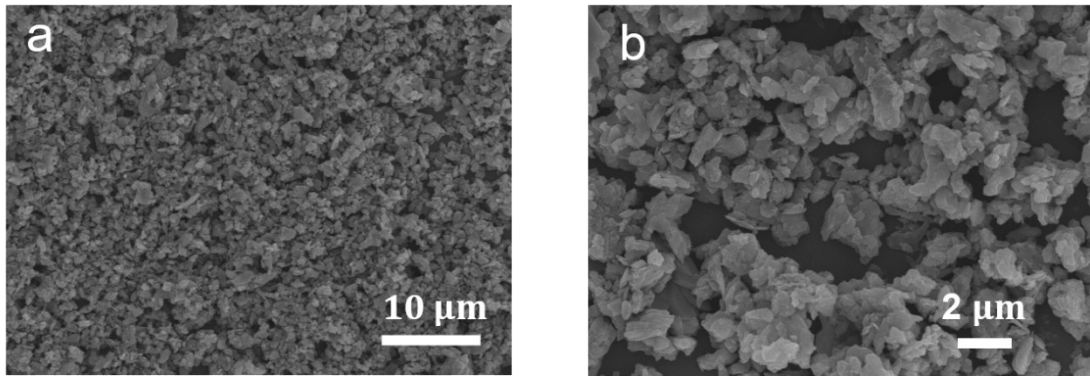


**Fig. S2.** SEM images of V-CSN powder.

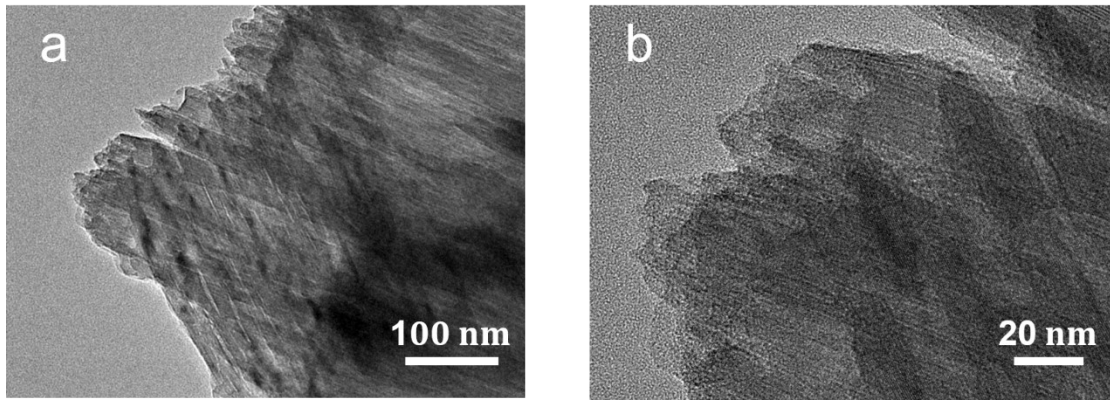


**Fig. S3.** TEM images of V-CSN powder.

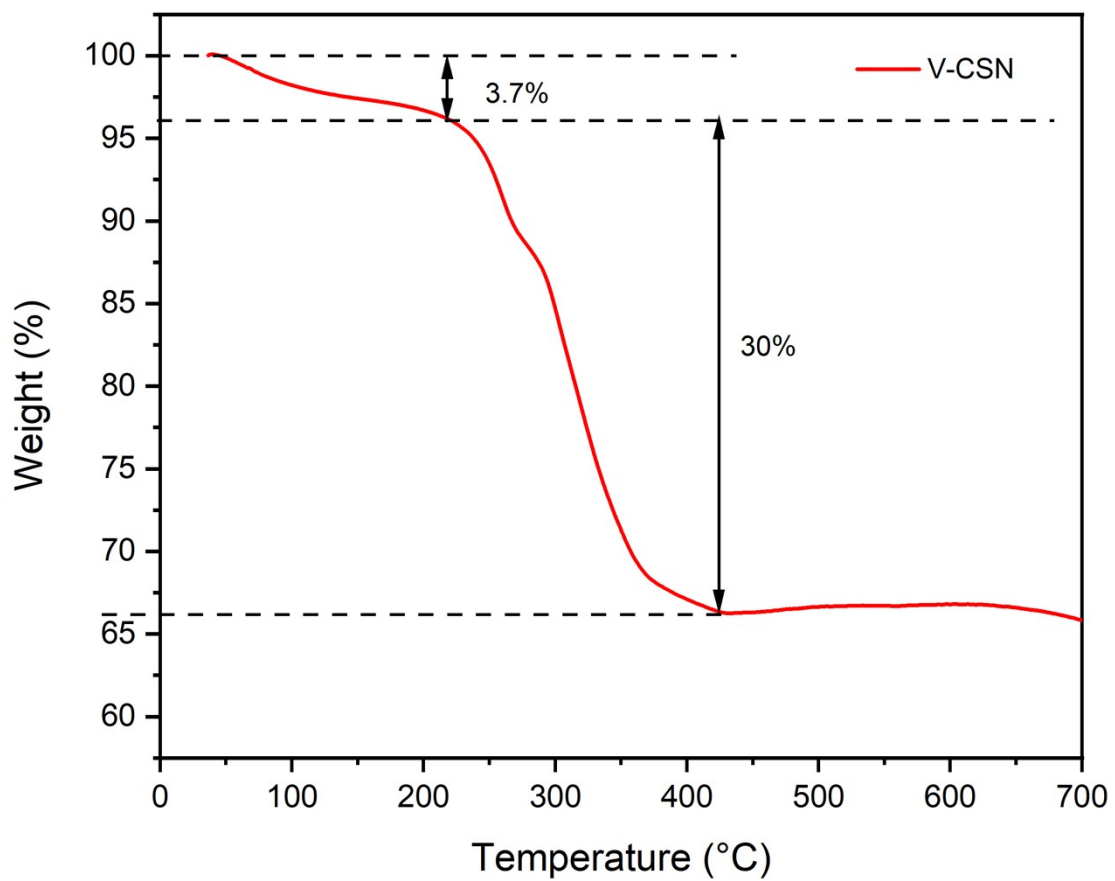


**Fig. S4.** Thermogravimetric analysis (TGA) of V-CSN under nitrogen atmosphere.

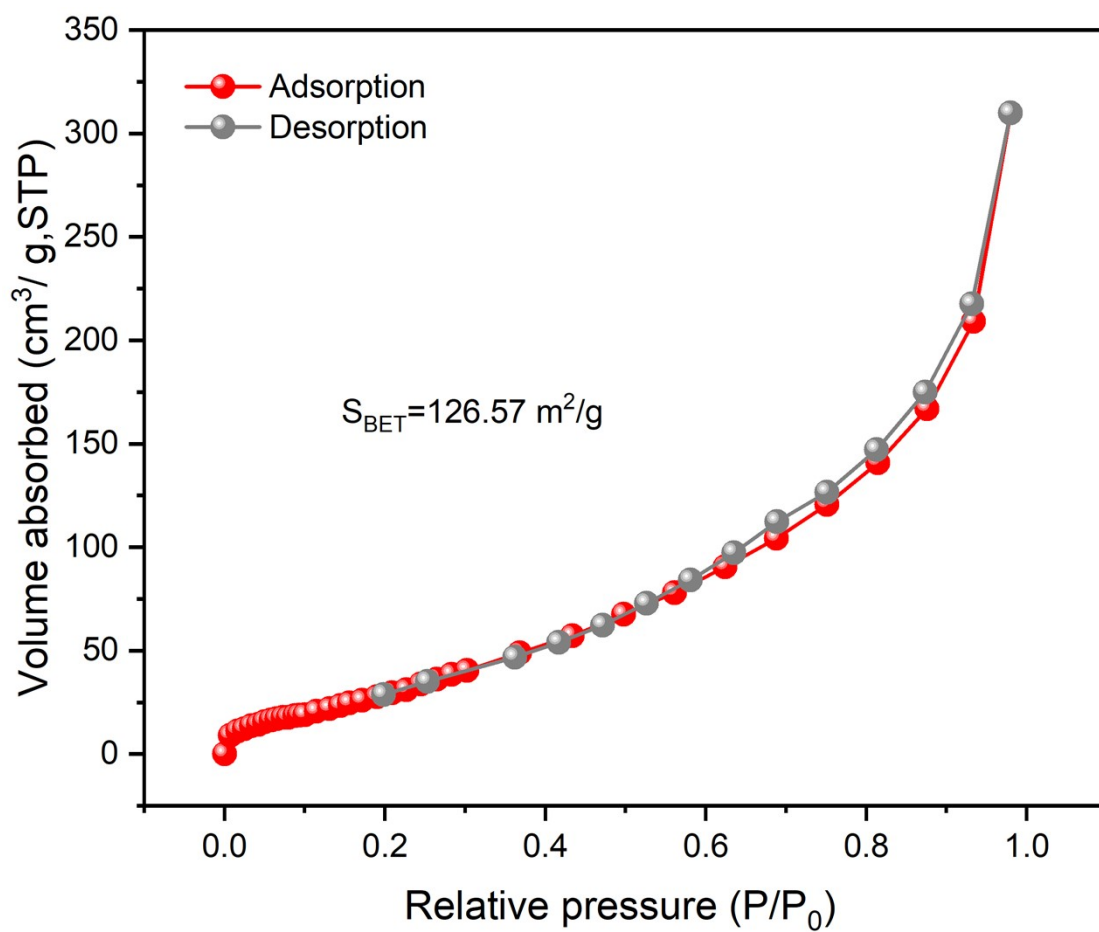


**Fig. S5.** Nitrogen adsorption/desorption isotherm plots of V-CSN powder.

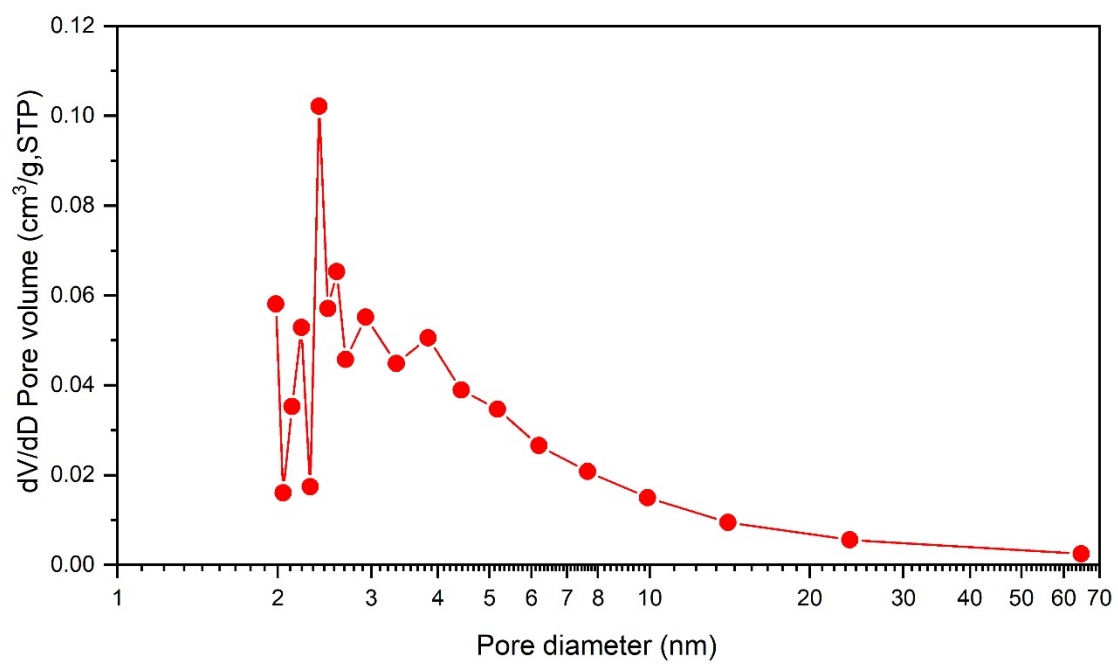


**Fig. S6.** Distribution diagram of BJH adsorption aperture of V-CSN powder.

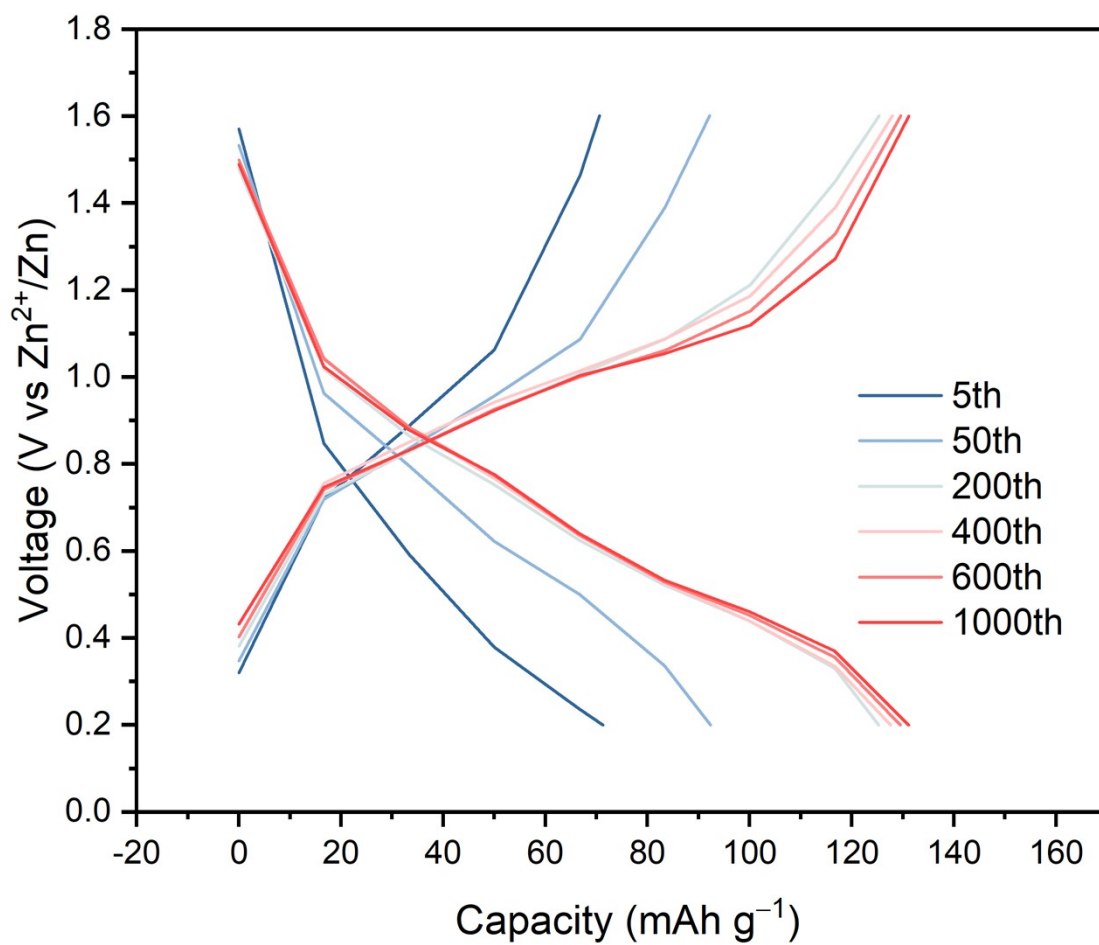


**Fig. S7.** GCD profiles of selected cycles at 2 A g<sup>-1</sup>.



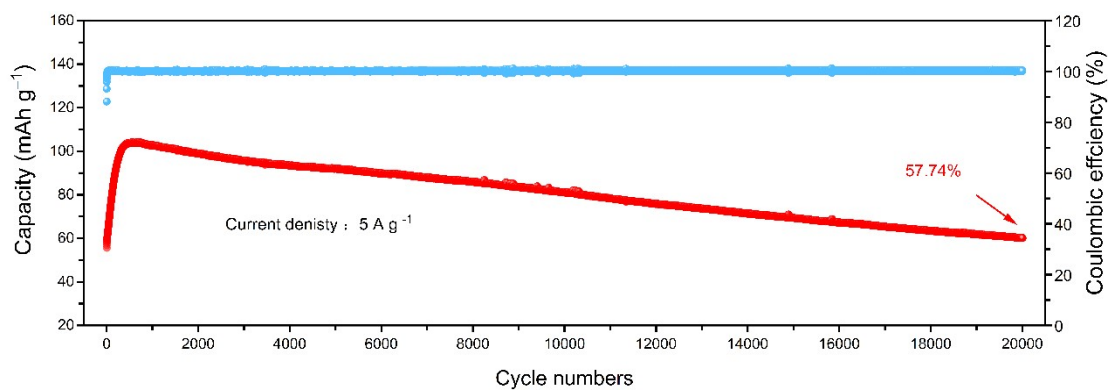


**Fig. S8.** Long cycling performance of V-CSN cathode at current densities of 5 A g<sup>-1</sup> (20,000 cycles).

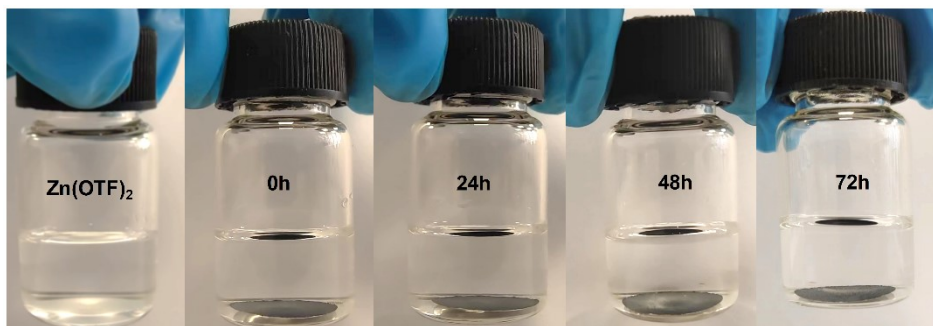


**Fig. S9** Optical images of V-CSN in 3 M Zn(OTF)<sub>2</sub> electrolyte for different time.

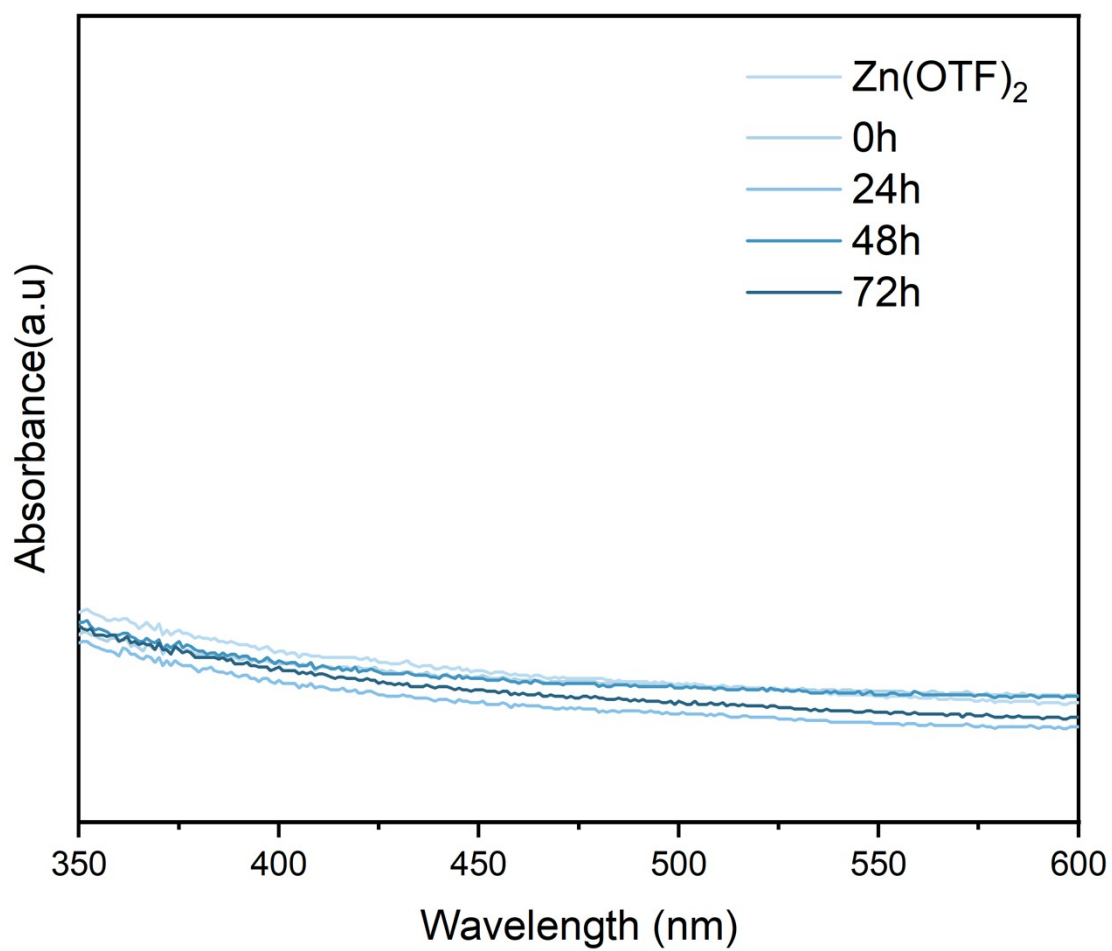


**Fig. S10** UV-vis spectra of V-CSN in 3 M Zn(OTF)<sub>2</sub> electrolyte for different time.

**Supplementary Table 1.** Comparison of main parameters and cycling property for this work with recently reported cathode materials of ZMBs.

cathode materials	Current density (A g <sup>-1</sup> )	Capacity retention (%)	Life (n)	Reference
V-CSN	5	82.3	8000	This work
C@multi-layer polymer	5	90.1	5000	1
FeMnHCF	1	85.30	1000	2
MnHCF	0.1	60.30	80	3
Cu <sub>3</sub> (HHTP) <sub>2</sub>	4	75.0	500	4
3DV <sub>2</sub> O <sub>5</sub>	5	90	4000	5
Al <sub>0.2</sub> V <sub>2</sub> O <sub>5</sub>	5	61.4	5000	6
V <sub>2</sub> O <sub>5</sub> @CNTs	5	72.0	6000	7
V <sub>2</sub> O <sub>3</sub> @C	5	78.0	2000	8
VO-Cr <sub>0.06</sub>	5	87.8	2000	9
Na <sub>4</sub> VMn(PO <sub>4</sub> ) <sub>3</sub>	5	89.1	3000	10
PANI	8	85.50	2000	11
TCNQ	5	93.3	5000	12
PTO	3	70.0	1000	13
TABQ	5	83.0	1000	14
TDT	10	81.3	3000	15

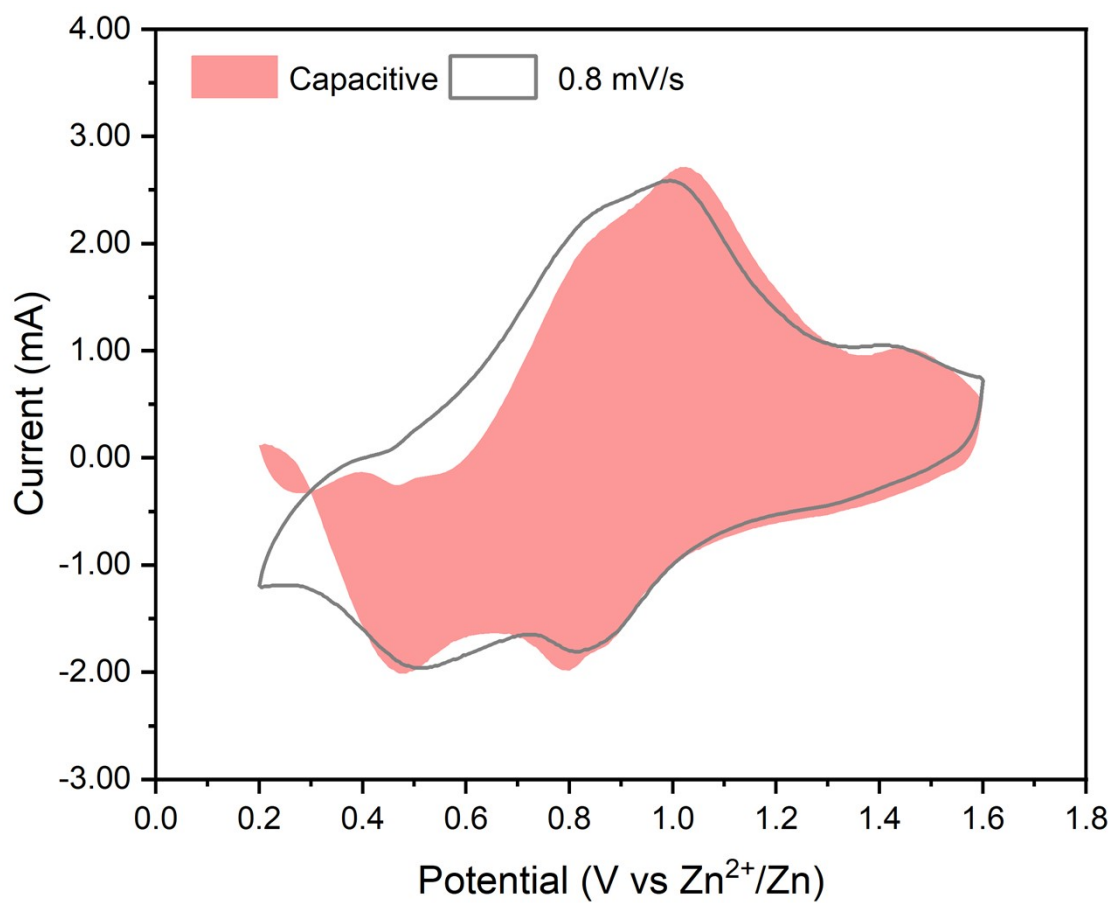


**Fig. S11.** Capacitive contribution of V-CSN cathode shown by shaded area at 0.8 mV s<sup>-1</sup>.

## Supplementary Note 1

The diffusion of zinc ions is determined by GITT, and the estimated value is according to formula (1):<sup>16, 17</sup>

$$D_{Zn^{2+}} = \frac{4L^2}{\pi\tau} \left( \frac{\Delta E_s}{\Delta E_t} \right)^2 \quad (1)$$

Where, L is the electrode thickness (cm), corresponding to the path length of ion diffusion;  $\tau$  is relaxation time;  $\Delta E_s$  stands for potential change caused by constant current pulse;  $\Delta E_t$  is the change in potential after removing the iR drop.

## Supplementary Note 2

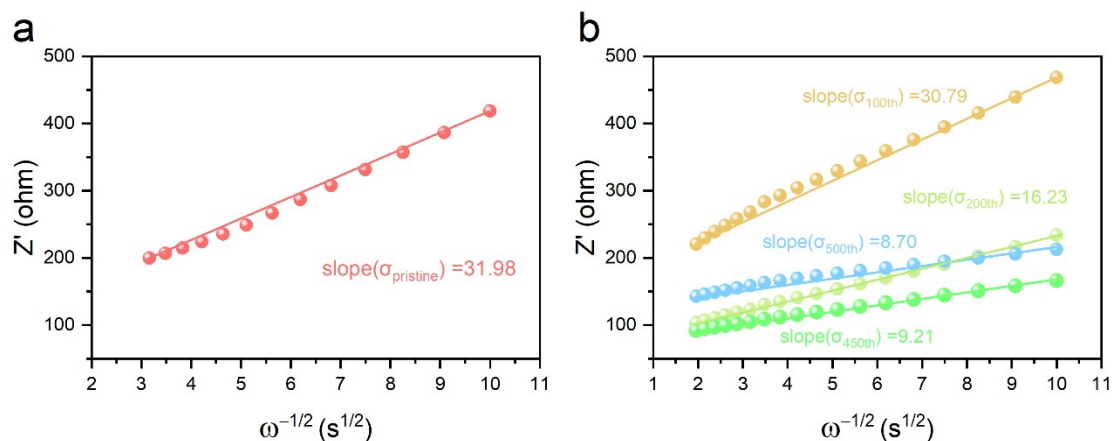


**Fig. S12.** The corresponding relationship between real part of impedance of V-CSN cathode and its low frequency region, (a) at pristine, (b) 100<sup>th</sup> cycles ,200<sup>th</sup> cycles, 450<sup>th</sup> cycles, 500<sup>th</sup> cycles.

The Nyquist diagram of V-CSN cathode cycle in different cycles is shown in the Fig.. The diffusion coefficient of zinc ions can be determined by the following two formulas. The first formula is to obtain the intermediate parameter  $\sigma$  according to the low frequency:<sup>17, 18</sup>

$$Z' = R_s + R_{ct} + \sigma \omega^{-1/2} \quad (2)$$

In the formula (2),  $Z'$  is the real impedance component,  $R_s$  the SEI resistance,  $R_{ct}$  the charge-transfer resistance,  $\sigma$  the Warburg factor and  $\omega$  the frequency.  $Z'$  is fitted linearly with  $\omega^{-1/2}$  in the low frequency region, where the slope of the curve corresponds to the value of  $\sigma$ . The  $\sigma$  coefficient of the pristine cathode is  $31.98 \Omega \text{ s}^{-1/2}$ , and the  $\sigma$  coefficient of 100, 200, 450, 500 cycles correspond to 30.79, 16.23, 9.13, 8.10  $\Omega \text{ s}^{-1/2}$  respectively. The diffusion coefficient is calculated by the following formula (3):

$$D_{\text{Zn}^{2+}} = \frac{R^2 T^2}{2 A^2 n^4 F^4 C^2 \sigma^2} \quad (3)$$

where  $D_{\text{Zn}^{2+}}$  is the diffusion coefficient of zinc ions,  $R$  is the molar gas constant,  $T$  the absolute temperature,  $A$  is the contact area between anode and electrolyte, the number

of electrons per molecule during oxidization,  $F$  is the Faraday constant, and  $C$  is the concentration of zinc ions. Since other values can be measured directly, we only need to substitute in the fitted value of  $\sigma$ .

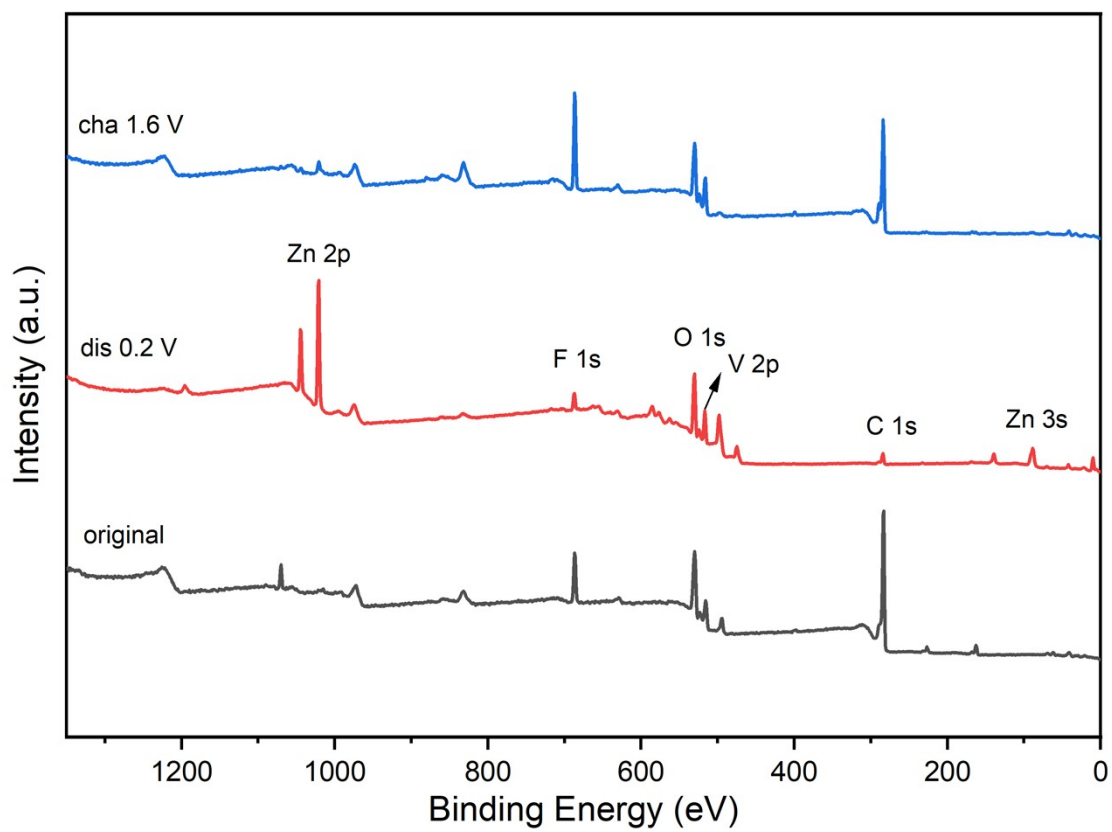


**Fig. S13.** A comprehensive survey of the XPS of with original state, fully discharge state (discharged to 0.2 V), fully charge state (charge to 1.6 V).



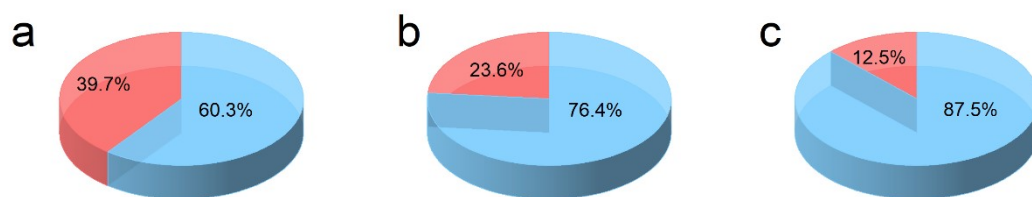


**Fig. S14.** The peak area percentage of V<sup>5+</sup> and V<sup>4+</sup> in the (a) original state, (b) fully discharge state (discharged to 0.2 V), and (c) fully charge state (charge to 1.6 V).

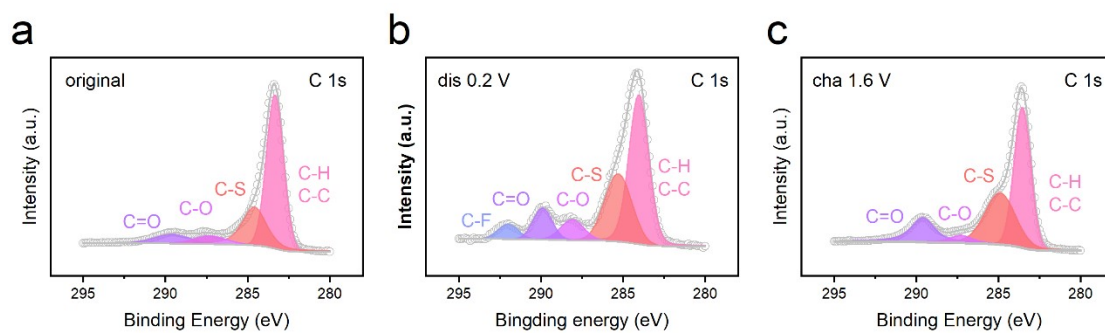


**Fig. S15.** Ex-situ high-resolution XPS spectra of C 1s with (a) original state, (b) fully discharge state (discharged to 0.2 V), and (c) fully charge state (charge to 1.6 V).

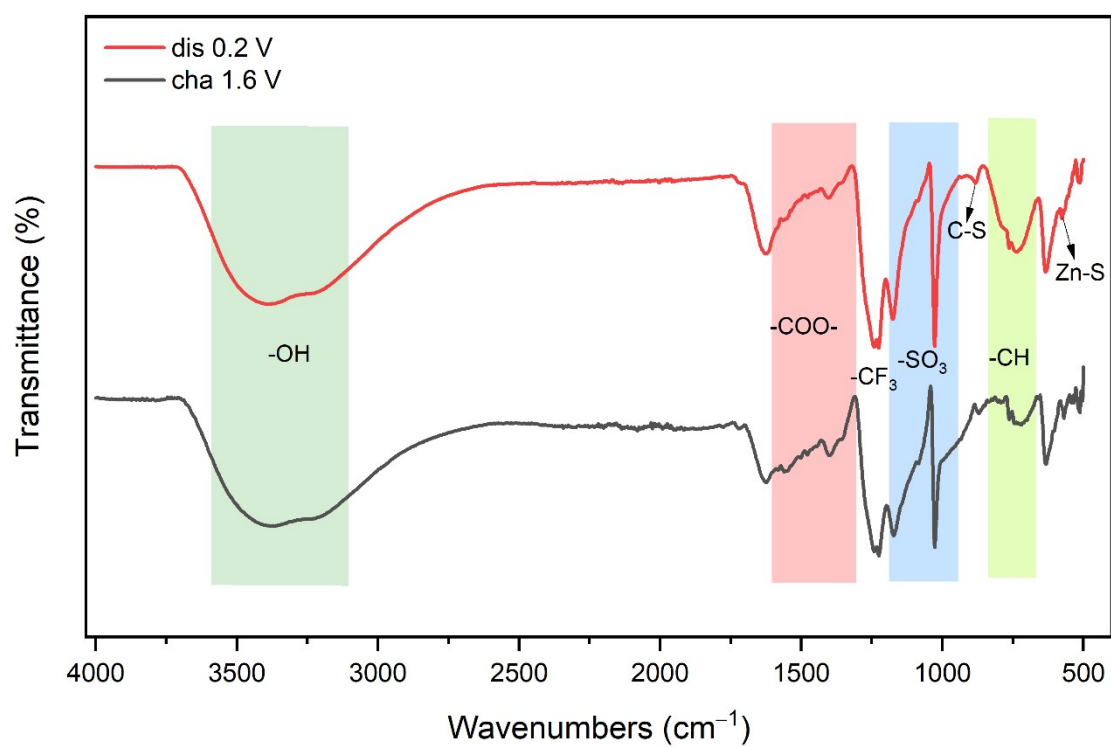


**Fig. S16.** Ex-situ FI-IR spectra of V-CSN cathode discharged to 0.2 V and charged to 1.6 V.

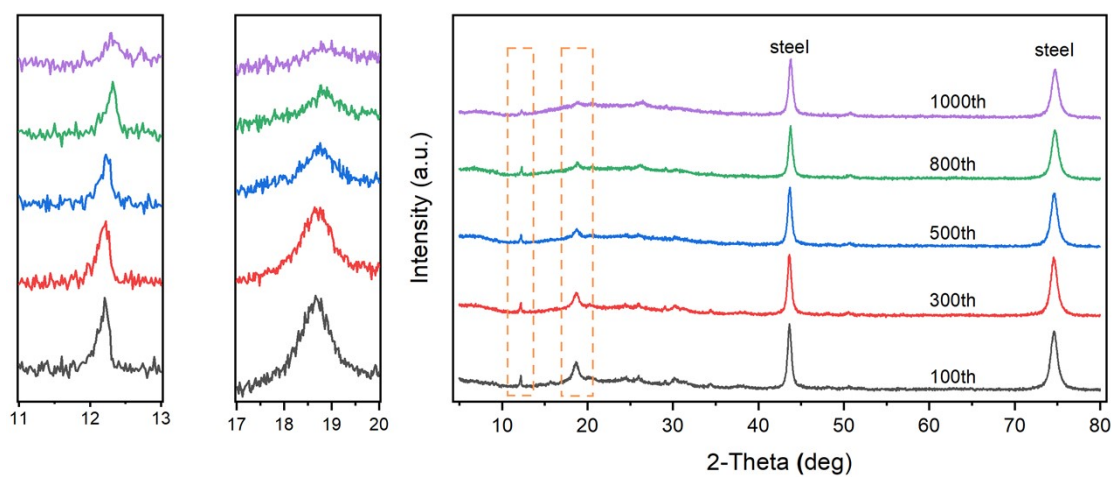


**Fig. S17.** Ex-situ XRD patterns of V-CSN cathodes at 100<sup>th</sup>, 300<sup>th</sup>, 500<sup>th</sup>, 800<sup>th</sup>, 1000<sup>th</sup> cycles.

### Supplementary Note 3

DFT Computational Methods: All the structures were reasonably optimized at a level of B3LYP-D3(BJ)/def2tzvp before simulations, remarkably in order to reduce the amount of computation, single coordination structure was selected as the calculation unit. All of the above calculations use water as solvation model. The frontier orbitals and molecular electrostatic potentials were visualized by Multiwfn and visual molecular dynamics (VMD version1.9.3).<sup>19-21</sup> The charge densities of V-CSN in different states were calculated through self-consistent field calculations. The adsorption energy was calculated with the equation (3):

$$E = E_{a-b} - (E_a + E_b) \quad (3)$$

where  $E$  is the adsorption energy, and  $E_{a-b}$  is the total energy of the relaxed a and b models at the equilibrium state.  $E_a$  and  $E_b$  are the calculation energy values of geometry-optimized.

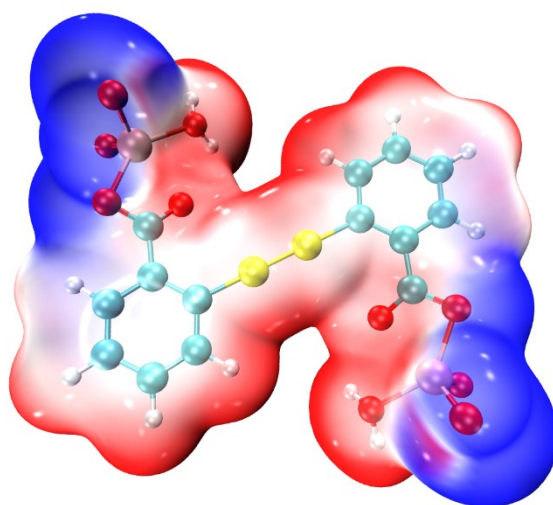


**Fig. S18.** The calculated MESP distribution of V-CSN with original state.

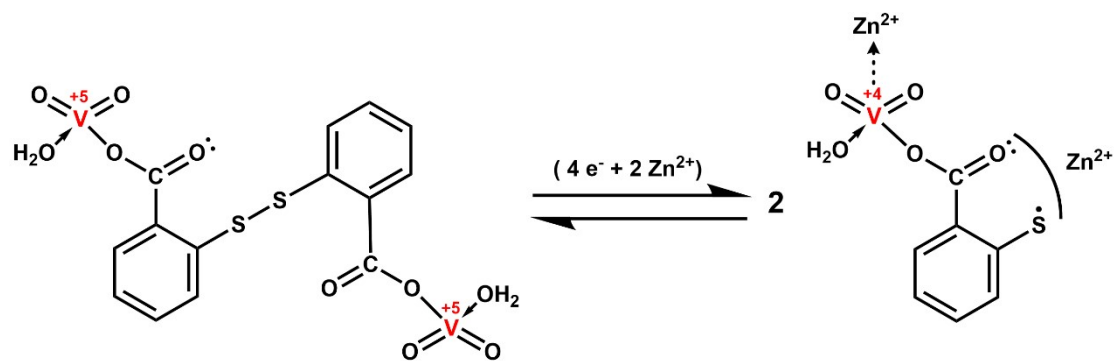


**Fig. S19.** Schematic diagram of the charge/discharge process in V-CSN cathode.

## Supplementary References

1. Y. Zhao, Y. Huang, F. Wu, R. Chen and L. Li, *Adv. Mater.*, 2021, **33**, 2106469.
2. D. Wang, C. Li, Q. Li, H. Li, J. Rehman, C. Zhi and L. Zhu, *Nano Energy*, 2022, **104**, 107990.
3. Y. Tan, H. Yang, C. Miao, Y. Zhang, D. Chen, G. Li and W. Han, *Chem. Eng. J.*, 2023, **457**, 141323.
4. K. W. Nam, S. S. Park, R. Dos Reis, V. P. Dravid, H. Kim, C. A. Mirkin and J. F. Stoddart, *Nat. Commun.*, 2019, **10**, 4948.
5. J. Zhu, L. Cao, Y. Wu, Y. Gong, Z. Liu, H. E. Hoster, Y. Zhang, S. Zhang, S. Yang, Q. Yan, P. M. Ajayan and R. Vajtai, *Nano Letters*, 2013, **13**, 5408-5413.
6. Q. Pang, W. He, X. Yu, S. Yang, H. Zhao, Y. Fu, M. Xing, Y. Tian, X. Luo and Y. Wei, *Appl. Surf. Sci.*, 2021, **538**, 148043.
7. H. Chen, H. Qin, L. Chen, J. Wu and Z. Yang, *J. Alloy. Compd.*, 2020, **842**, 155912.
8. D. Wang, W. Liang, X. He, Y. Yang, S. Wang, J. Li, J. Wang and H. Jin, *ACS Appl. Mater. Interfaces*, 2023, **15**, 20876-20884.
9. H. Yang, P. Ning, Z. Zhu, L. Yuan, W. Jia, J. Wen, G. Xu, Y. Li and H. Cao, *Chem. Eng. J.*, 2022, **438**, 135495.
10. Z. Wu, F. Ye, Q. Liu, R. Pang, Y. Liu, L. Jiang, Z. Tang and L. Hu, *Adv. Energy Mater.*, 2022, **12**, 2200654.
11. M.-Y. Zhang, Y. Song, X. Mu, D. Yang, Z. Qin, D. Guo, X. Sun and X.-X. Liu, *Small*, 2022, **18**, 2107689.
12. Z. Tie, L. Liu, S. Deng, D. Zhao and Z. Niu, *Angew. Chem. Int. Ed.*, 2020, **59**, 4920-4924.
13. Z. Guo, Y. Ma, X. Dong, J. Huang, Y. Wang and Y. Xia, *Angew. Chem., Int. Ed.*, 2018, **57**, 11737-11741.
14. Z. Lin, H.-Y. Shi, L. Lin, X. Yang, W. Wu and X. Sun, *Nat. Commun.*, 2021, **12**, 4424.



15. L. Lin, Z. Lin, J. Zhu, K. Wang, W. Wu, T. Qiu and X. Sun, *Energy Environ. Sci.*, 2023, **16**, 89-96.
16. X. Yang and A. L. Rogach, *Adv. Energy Mater.*, 2019, **9**, 1900747.
17. J. Kim, S. H. Lee, C. Park, H. S. Kim, J. H. Park, K. Y. Chung and H. Ahn, *Adv. Funct. Mater.*, 2021, **31**, 2100005.
18. P. Hu, T. Zhu, X. Wang, X. Wei, M. Yan, J. Li, W. Luo, W. Yang, W. Zhang, L. Zhou, Z. Zhou and L. Mai, *Nano Lett.*, 2018, **18**, 1758-1763.
19. S. Xu, F. Liu, J. Xu, Y. Cui and C. Wang, *J. Mol. Model.*, 2020, **26**, 111.
20. A. Ghysels, B. T. Miller, F. C. t. Pickard and B. R. Brooks, *J. Comput. Chem.*, 2012, **33**, 2250-2275.
21. Illinois, University of. Visual Molecular Dynamics. 2014.